NANOSEGREGATION PHENOMENA AT GRAIN BOUNDARIES OF METALLIC MATERIALS

Lejček P.[1], Janovec J.[2], Konečná R.[3]
[1]Institute of Physics, Academy of Sciences of the Czech Republic, Na Slovance 2, 182 21 Praha, Czech Republic,
[2]Slovak University of Technology, Faculty of Material Science and Technology, Dept. of Material Engineering, Bottova 23, 917 24 Trnava, Slovakia,
[3]University of Žilina, Faculty of Mechanical Engineering, Department of Materials Engineering, Univerzitná 1, 010 26 Žilina, Slovakia,
e-mail: pavel.lejcek@fzu.cz, jozef.janovec@stuba.sk, radomila.konecna@fstroj.utc.sk

NANOSEGREGAČNÍ JEVY NA HRANICÍCH ZRN KOVOVÝCH MATERIÁLŮ

Lejček P.[1], Janovec J.[2], Konečná R.[3]
[1]Fyzikální ústav, Akademie věd České republiky, Na Slovance 2, 182 21 Praha, ČR,
[2]Slovenská technická univerzita, Materiálovotechnologická fakulta, Katedra materiálového inžinierstva, Bottova 23, 917 24 Trnava, Slovensko,
[3]Žilinská univerzita, Strojnícka fakulta, Katedra materiálového inžinierstva, Univerzitná 1, 010 26 Žilina, Slovensko,
e-mail: pavel.lejcek@fzu.cz, jozef.janovec@stuba.sk, radomila.konecna@fstroj.utc.sk

Abstrakt

Hranice zrn značně ovlivňují vlastnosti polykrystalických materiálů používaných pro technické aplikace. Tento vliv je důsledkem rozdílné energie hranic zrn a objemu a následně důsledkem interakce hranic zrn s ostatními poruchami krystalové struktury, např. bodovými poruchami či dislokacemi, vedoucí k podstatnému snížení celkové Gibbsovy volné energie systému. Zejména jeden typ takové interakce – interakce hranic zrn s atomy příměsí (nanosegregace na hranicích zrn) – je velice významný neboť díky úzkému vztahu nanosegregace a interkrystalické koheze výrazně ovlivňují mechanické chování materiálů. Pro zlepšení mechanických vlastností technicky využívaných materiálů navrhl Tadao Watanabe v osmdesátých letech minulého století koncepci *Inženýrství hranic zrn*, která spočívá v produkci polykrystalických materiálů s optimálními vlastnostmi řízením charakteru a distribuce hranic zrn. Pro tuto moderní koncepci je však nezbytně nutná znalost co největšího rozsahu vlastností širokého spektra hranic zrn. Jednou z nejdůležitějších vlastností, které ovlivňují chování polykrystalických materiálů a která tak nutně musí být brána v úvahu v koncepci Inženýrství hranic zrn, je nanosegregace příměsí na hranicích zrn. Chemické složení jednotlivých hranic zrn může být určeno buď experimentálně pomocí nejrůznějších technik analýzy povrchů (např. AES, ESCA, SIMS) nebo simulováno metodami teoretického modelování, jako jsou Monte Carlo nebo molekulární dynamika. Oba tyto přístupy však mají vážná omezení, která nedovolují získání potřebných údajů pro rozsáhlé spektrum příměsí i hranic zrn. Proto je jakákoli předpověď takových dat velice perspektivní a žádoucí. Detailní analýza vlivu rozpustnosti příměsí v pevném stavu na Gibbsovu volnou energii segregace příměsí na hranicích zrn vedla k formulaci dvou vztahů. Prvním je tzv. *diagram segregace příměsí na hranicích zrn*,

$$\Delta H^0(\Phi, X_I^*) = \Delta H^*(\Phi, X_J^* = 1) + \nu R\left[T' \ln X_i^*(T')\right]$$

vztahující standardní molární entalpii segregace příměsi na hranicích zrn, ΔH_I^0, k údajům o rozpustnosti příměsi v pevném stavu, $T \leftarrow \ln X_I^*(T')$, a odrážející anisotropii segregace příměsí na hranicích zrn, $\Delta H_I^*(\Phi, X_I^*=1)$. Druhá závislost, tzv *kompenzační jev mezi entalpií a entropií*, ukazuje úzký vztah mezi standardní molární entalpií, ΔH_I^0, a standardní molární entropií, ΔS_I^0, segregace příměsi na hranicích zrn,

$$\Delta S_I^0 = \frac{\Delta H_I^0}{T_c} + \sigma_p \,.$$

Na základě těchto dvou vztahů lze předpovědět segregaci libovolné příměsi na libovolné hranici zrn v α-železe. Tato předpověď, která poskytuje podstatné rozšíření databáze o segregaci příměsí na hranicích zrn, je testována porovnáním výsledků experimentálního měření segregace na hranicích zrn v polykrystalických materiálech binárních, pseudobinárních a mnohosložkových systémů. Její perspektiva je rovněž ukázána na příkladu předpovědi chemického složení hranic zrn ve dvou technicky používaných materiálech: nízkolegované feritické oceli a feritické fázi litiny s kuličkovým grafitem. Díky zcela obecnému odvození výše uvedených vztahů může být naše metoda predikce snadno rozšířena na různé základní materiály a různá rozhraní, např. volné povrchy či fázová rozhraní.

Abstract

Grain boundaries strongly influence the properties of polycrystalline materials, which are used for practical applications. This effect originates from the energy difference between the internal interfaces and the crystal volume, and consequently, from an interaction of the grain boundaries with other lattice defects such as point defects and dislocations, resulting in substantial reduction of the total Gibbs free energy of the system. One representative of such interaction – the interaction with the solute atoms (nanosegregation at the grain boundaries) – is of high importance because it predominantly affects the intergranular cohesion and, in consequence, the mechanical behavior of the materials. To improve the mechanical properties of the technically used materials, the concept of *Grain Boundary Engineering* was proposed in 1980s by Tadao Watanabe to produce the polycrystals with optimum properties by controlling the grain boundary character distribution. For this purpose, the knowledge of the broad spectrum of properties of the broad spectrum of grain boundaries is needed. One of the most important properties which affects the behavior of polycrystalline materials and which has thus be considered in the Grain Boundary Engineering concept, is the nanosegregation of the solutes at the grain boundaries. The chemical composition of individual grain boundaries can be either measured experimentally using various techniques of surface analysis (for example AES, ESCA and SIMS), or simulated by the methods of theoretical modeling (for example Monte Carlo and molecular dynamics). Both these approaches, however, have serious limitations, which do not allow providing us with the data for a broad spectrum of the solutes and for a broad spectrum of the grain boundaries. Therefore, any prediction of such data seems to be very prospective and desirable. A detail analysis of the effect of the solid solubility on variations of the Gibbs free energy of interfacial segregation resulted in formulation of two simple expressions. One of them is the so-called *grain boundary segregation diagram*,

$$\Delta H^0(\Phi, X_I^*) = \Delta H^*(\Phi, X_J^*=1) + vR\left[T' \ln X_i^*(T')\right]$$

relating the standard molar enthalpy of solute segregation, ΔH_I^0, to the solid solubility data, $T \leftarrow \ln X_I^*(T')$, and reflecting anisotropy of grain boundary segregation, $\Delta H_I^*(\Phi, X_I^*=1)$. The other

expression, so-called the *enthalpy-entropy compensation effect* shows a close relationship between the standard molar enthalpy, ΔH_I^0, and the standard molar entropy, ΔS_I^0, of grain boundary segregation,

$$\Delta S_I^0 = \frac{\Delta H_I^0}{T_c} + \sigma_p \cdot$$

Based on the above two relationships the segregation of any solute at any grain boundary of α-iron can be predicted. This prediction, which offers a substantial extension of the database on grain boundary segregation is tested by comparing with the literature data on experimental measurement of grain boundary segregation in polycrystalline materials of binary, pseudobinary or multicomponent systems. In addition, the potency of the prediction method is shown to display chemical composition of the grain boundaries in two technically used materials, the low-alloy ferrite steel and the ferrite phase of the nodular cast iron. Due to the generality of the derivation of the above relationships, the proposed prediction method can be simply extended to different matrices and types of the interfaces (free surfaces, phase interfaces).

Keywords: segregation, grain boundaries, prediction, thermodynamics, ferrite alloys

Introduction

Structural defects influence the properties of materials. For example, interaction between dislocations and fine precipitates during forming and thermomechanical treatment give rise to strengthening of metals and alloys. One of the most important classes of defects affecting the microstructure of polycrystals are internal interfaces and especially, *grain boundaries* separating adjacent grains. The bonds between individual atoms in the grain boundary are altered as compared to the bulk crystal [1]. Grain boundaries thus possess higher energy and consequently, different properties than the crystal interior. Since the grain boundaries in polycrystals create a three-dimensional "web" spread throughout the material and thus represent a self-standing link in material structure with different mechanical, electric and magnetic properties, they substantially contribute to the behaviour of the material. Let us emphasise that the properties of grain boundaries are usually worse than those of the crystal interior. It significantly limits possibilities for practical applications of polycrystalline materials. Moreover, the grain boundaries show the tendency to reduce the total energy of the system by interaction with other lattice defects, such as solute atoms. It results in accumulation (*segregation*) of the solute atoms at the grain boundaries to such extent that the interfaces – compared to the bulk – may become qualitatively different in chemical nature. Chemical changes at the grain boundaries may induce degradation processes in the alloys, e.g. intergranular embrittlement [2].

Grain boundary segregation is a very important phenomenon, which affects the behaviour of polycrystals to a large extent. This phenomenon covers all concentration changes at a grain boundary supposing the character of a solid solution is preserved [2]. It is worth noting that the limit of solubility of a solute in a basic material (matrix) may differ at grain boundaries and in bulk crystal [3]. If particles of another phase appear at the grain boundaries one must call it grain boundary precipitation. Grain boundary precipitation is continuation of grain boundary segregation, indeed, because new particles grow at the interface due to supersaturation of the solid solution at the grain boundary [4].

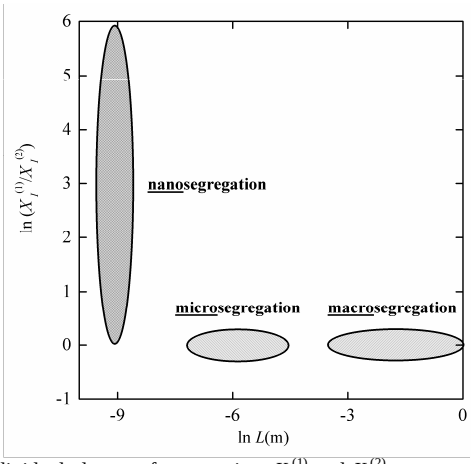

Fig.1 Schematic depiction of individual classes of segregation. $X_I^{(1)}$ and $X_I^{(2)}$ represent the concentrations of individual compared regions, L represents the length scale of the effect. Macro- and microsegregation are connected with the liquation effects while nanosegregation represents the grain boundary segregation

Let us mention that the term *segregation* is used in metallurgy to describe a wide range of phenomena. We can meet this term often in relation to solidification processes. During solidification of a molten alloy, concentration differences occur in the cast due to the liquation. The liquation effects can embrace areas of "meter" scale in the cast and of "micrometer" scales between dendrites and interdendrite space. The former effect is referred to as *macrosegregation*, the latter effect to as *microsegregation* [5]. In contrast the grain boundary segregation concerns one or several atomic layers and is controlled by grain boundary energy. Thus, it may be ultimately limited to " nanometer" scale. On the other hand, it can exhibit much larger concentration differences than macro- or microsegregations (Fig. 1). From the point of view of the above scale-based classification, the grain boundary segregation can be called *nanosegregation*.

Thermodynamics of equilibrium grain boundary segregation

As mentioned above, the grain boundary segregation is thermodynamically favourable process, which leads to accumulation of solute atoms at the grain boundary. The term *equilibrium grain boundary segregation* is used to denote the very local redistribution of solutes at grain boundaries caused by *minimisation of the total Gibbs free energy of the system*. It is supposed that chemical potentials μ_i of all species involved in solid solution are constant throughout the system. At equilibrium there is partitioning which results in grain boundary enrichment by surface-active species. The level of the enrichment is defined by the system parameters at equilibrium only and not by the alloy history, and can be reproduced by re-establishing the identical physicochemical conditions.

A detail thermodynamic analysis [6,7] shows that the grain boundary segregation can be described as exchange of solute I and matrix M elements between grain boundary Φ and bulk B,

$$I^B + M^\Phi \Leftrightarrow I^\Phi + M^B \tag{1}$$

The basic condition for equilibrium between the grain boundary and bulk is

$$\mu_I^B + \mu_M^\Phi = \mu_I^\Phi + \mu_M^B \tag{2}$$

for each component i ($i = I, M$). Accepting the general expression for chemical potentials, $\mu_i = \mu_i^0 + RT \ln a_i$, where a_i is the activity of the element i in a solid solution [8], we can write

$$\frac{a_I^\Phi}{a_M^\Phi} = \frac{a_I^B}{a_M^B} \exp\left(-\frac{\Delta G_I^0}{RT}\right) \tag{3}$$

In eq. (3), the *standard* molar Gibbs free energy of segregation,

$$\Delta G_I^0 = (\mu_I^{0,\Phi} - \mu_I^{0,B}) - (\mu_M^{0,\Phi} - \mu_M^{0,B}) = \Delta H_I^0 - T\Delta S_I^0 \tag{4}$$

is defined as combination of the standard chemical potentials of the pure elements I and M at the grain boundary and in the bulk, $\mu_i^{0,\Phi}$ and $\mu_i^{0,B}$, respectively, at the temperature and pressure of the system. ΔH_I^0 and ΔS_I^0 are the standard molar enthalpy and entropy of segregation of solute I at the grain boundary in matrix M. The chemical potentials referring to the grain boundary, $\mu_i^{0,\Phi}$, intrinsically involve the contribution of the grain boundary energy, σ^Φ [6,7],

$$\mu_i^{0,\Phi} = \xi_i^{0,\Phi} - \sigma^\Phi A_i \tag{5}$$

where A_i is the partial molar area of species i at the grain boundary, and $\xi_i^{0,\Phi}$ is the partial molar Helmholz free energy of species i in the interface in the standard state.

Since generally, $a_i = \gamma_i X_i$, where γ_i is the activity coefficient of element i, [8], we can rewrite eq. (3) using $X_M = 1 - \sum_{J=1}^{M-1} X_J$ as

$$\frac{X_I^\Phi}{1 - \sum_{j \neq M} X_j^\Phi} = \frac{X_I}{1 - \sum_{j \neq M} X_j} \exp\left(-\frac{\Delta G_I^0 + \Delta G_I^E}{RT}\right) \tag{6}$$

In eq. (6),

$$\Delta G_I^E = RT \ln \frac{\gamma_I^\Phi \gamma_M^B}{\gamma_M^\Phi \gamma_I^B} \tag{7}$$

is the *excess* molar Gibbs free energy of segregation. Eq. (6) represents the *general thermodynamic form of the segregation isotherm*. Since the values of the activity coefficients in eq. (7) are not known, ΔG_I^E is presently correlated according to models, which are based on semiempirical approaches. The simplest approach supposing ideal behaviour of all components in the system (i.e. $\Delta G_I^E = 0$) is called *Langmuir–McLean segregation isotherm* [9]. It can be expressed for a binary system as

$$\frac{X_I^\Phi}{1 - X_I^\Phi} = \frac{X_I}{1 - X_I} \exp\left(-\frac{\Delta G_I^0}{RT}\right) \tag{8}$$

Regular solid solution model results in *Fowler isotherm* (in case of a binary system) and in *Guttmann isotherm* (for multicomponent systems) [2,4,7,9].

Effect of interfacial energy on grain boundary segregation

There are many examples of experimental as well as theoretical evidence of the effect of various thermodynamic and structural variables (pressure, magnetic field, grain boundary structure, character of both solute and matrix elements) on grain boundary segregation [9]. It is apparent from eqs. (4) and (6) that the influence of individual parameters on grain boundary segregation is primarily involved in variations of the values of ΔG_I^0 and consequently, of the values of ΔH_I^0 and ΔS_I^0. Additionally, temperature affects the values of the exponential term in eq. (6). The effect of bulk concentration on grain boundary segregation is also evident from eq. (6). All above-mentioned effects as well as grain boundary composition contribute to variations of the values of ΔG_I^E in real systems. Let us now discuss one of these effects, the effect of the grain boundary energy.

The variations of the standard molar Gibbs free energy of segregation, ΔG_I^0, can be expressed by its total differential,

$$\mathrm{d}\Delta G_I^0 = \left(\frac{\partial \Delta G_I^0}{\partial T}\right)_{P,\Omega_i} \mathrm{d}T + \left(\frac{\partial \Delta G_I^0}{\partial P}\right)_{T,\Omega_i} \mathrm{d}P + \sum_j \left(\frac{\partial \Delta G_I^0}{\partial \Omega_j}\right)_{T,P,\Omega_{i\neq j}} \mathrm{d}\Omega_j \tag{9}$$

In eq. (9), Ω_j are the intensive variables of the system such as magnetic field and grain boundary energy [10]. It is apparent that $(\partial \Delta G_I^0/\partial P)_{T,\Omega} = \Delta V_I^0$ (ΔV_I^0 is the standard molar segregation volume of solute *I*) and $(\partial \Delta G_I^0/\partial T)_{P,\Omega} = -\Delta S_I^0$ [8]. In agreement with eq. (4), the total differentials of the standard molar enthalpy and entropy of segregation can be expressed analogously,

$$\mathrm{d}\Delta H_I^0 = \sum_j \left(\frac{\partial \Delta H_I^0}{\partial \Omega_j}\right)_{T,P,\Omega_{i\neq j}} \mathrm{d}\Omega_j \quad \text{and} \quad \mathrm{d}\Delta S_I^0 = \sum_j \left(\frac{\partial \Delta S_I^0}{\partial \Omega_j}\right)_{T,P,\Omega_{i\neq j}} \mathrm{d}\Omega_j \tag{10}$$

The changes in the grain boundary energy σ affect the values of the chemical potentials of the solute and matrix element at the grain boundary (cf. eq. (5)) and thus, the standard molar Gibbs free energy of segregation. The changes of the grain boundary energy σ may be of different nature but principally, σ changes due to (i) *grain boundary structure* (anisotropy of grain boundary segregation), and (ii) *nature of segregating and matrix elements*.

Structural dependence of grain boundary segregation can be displayed as an orientation dependence of ΔH_I^0 [11]. An example of the anisotropy of solute segregation at grain boundaries of α-iron is shown in Fig. 2. On the other hand, the dependence of the grain boundary segregation on the nature of the solute can be represented by the dependence of ΔH_I^0 on the solubility of the solute in solid matrix, $X_I^*(T)$ [12], as shown in Fig. 3. In fact, this representation is similar to that between the grain boundary enrichment ratio and the solid solubility revealed earlier by Hondros and Seah [13].

Chemical potential, μ_I^*, of the solute *I* in saturated bulk solid solution is

$$\mu_i^* = \mu_i^0 + RT \ln a_i^* \tag{11}$$

where a_I^* is the activity of the solute *I* in the system *M–I* at the solubility limit $X_I^*(T)$ [14]. Providing the saturated bulk solid solution of *I* in *M* is considered as another standard state, the segregation free energy of the solute *I*, ΔG_I^*, can be expressed as

$$\Delta G_I^* = (\mu_I^{0,\Phi} - \mu_I^{0,B}) - (\mu_M^{*,\Phi} - \mu_M^{0,B}) = \Delta G_I^0 - RT \ln a_I^* \tag{12}$$

It can be simply shown that

$$\Delta S_I^* = \Delta S_I^0 - R\left(\frac{\partial\left[T \ln a_I^*\right]}{\partial T}\right)_{P,X_j} \tag{13}$$

As the product on the right-hand side of eq. (13), $T \ln a_I^* = \Delta G_I^{sol}/R$, was proved to be nearly independent of temperature for various systems [13,14], the term in brackets of eq. (13) is negligible. Consequently, both entropy terms in eq. (13) are equal. Eq. (12) can be then rewritten as

$$\Delta H_i^0 = \Delta H_i^* + RT \ln a_i^* \tag{14}$$

The plot of numerous pairs of the values of activities and corresponding concentrations at the solid solubility level in various systems found in [15] revealed a simple power relationship between these two values for different systems and temperatures [14],

$$a_i^* = (X_i^*)^v \tag{15}$$

where the parameter v depends on matrix element M albeit not on the nature of the solute element I [14]. A combination of eqs. (14) and (15) provides us with [14]

$$\Delta H^0(\Phi, X_I^*) = \Delta H^*(\Phi, X_J^* = 1) + vR\left[T' \ln X_i^*(T')\right] \tag{16}$$

Eq. (16) represents a very important relationship between the standard molar enthalpy of segregation of a solute element with solid solubility X_I^* (at a temperature T') and the product of logarithm of solid solubility and corresponding temperature. Let us emphasise that the product $T'\ln X_I^*(T') \approx const.$ and therefore, ΔH^0 (Φ, X_I^*) is independent of temperature. As was discussed above, ΔH_I^0 depends on the grain boundary structure. This dependence is included in $\Delta H_J^*(\Phi)$ representing the standard molar enthalpy of segregation of a solute with unlimited solid solubility, $X_J^* = 1$. It is apparent that the "structural" term $\Delta H^*(\Phi)$ is *independent* of solid solubility and the "solubility" term $vR[T'\ln X_I^*(T')]$ *does not depend* on grain boundary energy [14]. This conclusion can be well seen from the plot of ΔH^0 vs. misorientation angle θ and vs. $[T'\ln X_I^*(T')]$ so-called *grain boundary segregation diagram* [14,16] (Fig. 4): the lines joining the segregation enthalpy of individual solute elements at corresponding grain boundaries are parallel.

Eq. (16) and the grain boundary segregation diagram represent an extension of the model of Hondros and Seah [13] by considering segregation anisotropy ($\Delta H_I^0 = f(\Phi)$) and non-ideal behaviour of the solid solutions at solubility limit ($v \neq 1$) [14].

In sense of eq. (10), we can write

$$\mathrm{d}\Delta H_I^0 = \left(\frac{\partial \Delta H_I^0}{\partial \sigma^\Phi}\right)_{T,P,\Omega_i \neq \sigma^\Phi} \mathrm{d}\sigma^\Phi + \left(\frac{\partial \Delta H_I^0}{\partial \sigma_I}\right)_{T,P,\Omega_i \neq \sigma_I} \mathrm{d}\sigma_I \tag{17}$$

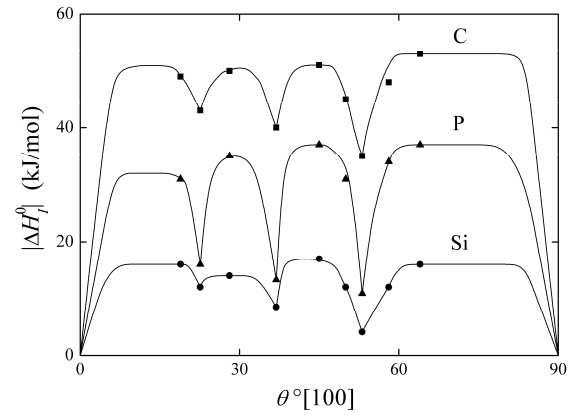

Fig.2 Dependence of enthalpy of segregation of silicon, phosphorus and carbon on misorientation angle of [100] symmetrical grain boundaries [11]

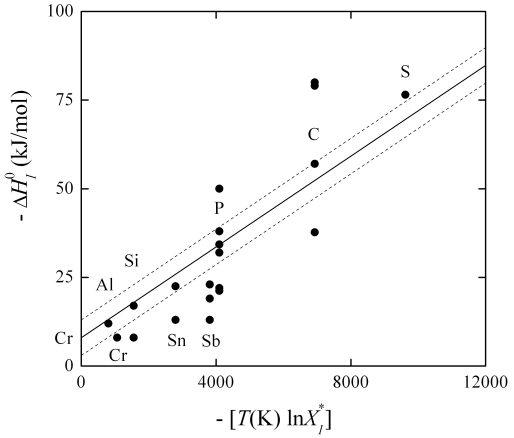

Fig.3 Dependence of enthalpy of segregation of various solutes at general grain boundaries on solid solubility data of α-iron. Full line depicts the prediction (cf. eq. (16)); the scatter of ±5 kJ/mol from the prediction is marked by the dashed lines [12]

where σ^{Φ} and σ_I reflect the changes of the grain boundary energy caused by changes in structure and nature of the solute, respectively. The total differential of the segregation entropy can be expressed analogously. Evidently, ranges of the values of σ^{Φ} and σ_I must exist, for that a constant temperature T_c is defined as [17]

$$T_c = \frac{\mathrm{d}\Delta H_I^0}{\mathrm{d}\Delta S_I^0} = \frac{\left(\frac{\partial \Delta H_I^0}{\partial \sigma^{\Phi}}\right)_{T,P,\Omega_i \neq \sigma^{\Phi}} \mathrm{d}\sigma^{\Phi} + \left(\frac{\partial \Delta H_I^0}{\partial \sigma_I}\right)_{T,P,\Omega_i \neq \sigma_I} \mathrm{d}\sigma_I}{\left(\frac{\partial \Delta S_I^0}{\partial \sigma^{\Phi}}\right)_{T,P,\Omega_i \neq \sigma^{\Phi}} \mathrm{d}\sigma^{\Phi} + \left(\frac{\partial \Delta S_I^0}{\partial \sigma_I}\right)_{T,P,\Omega_i \neq \sigma_I} \mathrm{d}\sigma_I} \tag{18}$$

i.e.,

$$T_c \mathrm{d}\Delta S_I^0 = \mathrm{d}\Delta H_I^0 \tag{19}$$

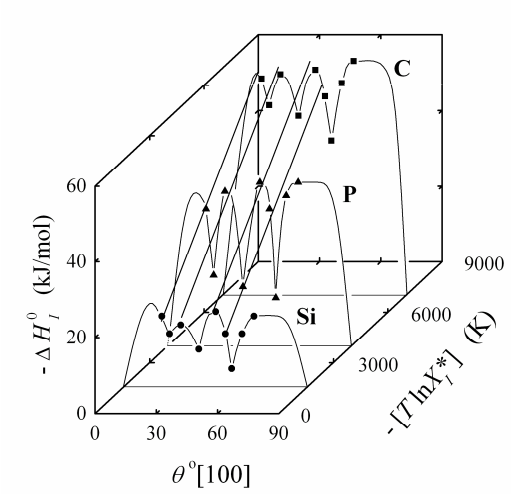

Fig.4 Grain boundary segregation diagram for [100] symmetrical tilt grain boundaries in α-iron [14]

It follows from eqs. (4), (18) and (19) that

$$\mathrm{d}\Delta G_I^0(T_c) = \left(\frac{\partial \Delta G_I^0}{\partial \sigma^\Phi}\right)_{P,\Omega_i \neq \sigma^\Phi} \mathrm{d}\sigma^\Phi + \left(\frac{\partial \Delta G_I^0}{\partial \sigma_I}\right)_{P,\Omega_i \neq \sigma_I} \mathrm{d}\sigma_I = 0 \tag{20}$$

Integration of eq. (19) provides $\Delta H_I^0 = T_c(\Delta S_I^0 + \Delta S')$ and thus,

$$\Delta S_I^0 = \frac{\Delta H_I^0}{T_c} - \frac{\Delta G^0(T_c)}{T_c} \tag{21}$$

Therefore, $\Delta G_I^0(T_c) = T_c \Delta S'$ which is constant according to eq. (20), i.e., independent of any change of the grain boundary energy at T_c. Eq. (18) represents the *compensation effect* suggesting that the change of the standard molar enthalpy of segregation, $\mathrm{d}\Delta H_I^0$, caused by the change of the grain boundary energy, is *compensated* by the corresponding change of the standard molar entropy of segregation, $\mathrm{d}\Delta S_I^0$ in a linear way despite of the nature of the changes of the grain boundary energy. T_c is the compensation temperature [17]. $\Delta S' = \Delta G_I^0(T_c)/T_c$ is the negative configuration entropy at T_c [18] and is independent either of the grain boundary structure or the nature of the segregated solute. Let us mention that the compensation effect is completely general and holds for all considered variables Ω_j in sense of eqs. (9) and (10) [17]. It is also worth noting that condition (20) does not represent an equilibrium condition and thus, no transformation can generally occur at T_c.

The compensation effect for grain boundary segregation in α-iron is shown in Fig. 5. It is seen that there exist two branches of the dependence ΔS_I^0 vs. ΔH_I^0. It is because the compensation effect may exist for the process only, the nature and mechanism of which remain the same when a variable changes. However, the segregation occurs either on substitution or at interstitial positions, representing different mechanisms. In Fig. 5, the upper and lower lines

correspond to segregation at interstitial and substitution positions, respectively, but possess the same slope. It means that the compensation temperature is independent of the mechanism of the segregation (T_c = 930 K). Therefore, we may well accept that T_c is a characteristic parameter of the matrix element. $\Delta S'$ is different for both branches, indeed [17].

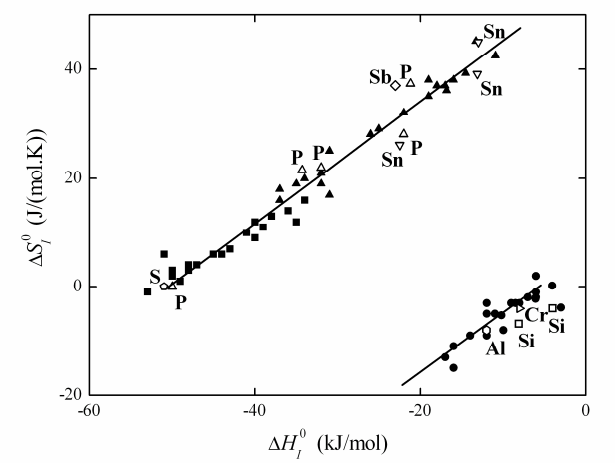

Fig.5 Compensation effect for segregation in α-iron. Full symbols – data for segregation of carbon (squares), phosphorus (triangles) and silicon (circles) at individual grain boundaries [11]. Empty symbols – data from literature measured for solute segregation in polycrystalline α-iron [12]

Let us notice that the above-demonstrated thermodynamic derivation of the compensation effect was performed generally and can be applied to any thermodynamic process or equilibrium state that is characterised by changes of the Gibbs free energy despite of its meaning as characteristic equilibrium change or activation energy. This is documented by observing the compensation effect not only in various interfacial processes and states (e.g. grain boundary diffusion, migration, segregation) but also in many fields of physics, chemistry, biology, medicine etc. [17].

Prediction of grain boundary segregation

Thermodynamic considerations resulting in eqs. (16) and (21) were already used for prediction of grain boundary segregation [12,19]. For this prediction, few parameters are needed only: $\Delta H_I^*(\Phi)$, v, T_c, and $\Delta S'$. The value of $\Delta S'$ reflects the mechanism of grain boundary segregation (at substitution and interstitial sites). For grain boundary segregation in α-iron, these parameters are listed in Table 1. A knowledge of the solubility of the solute I in the M–I solid solution, $X_I^*(T')$, is only necessary to determine the values of $\Delta H_I^0(\Phi)$ and $\Delta S_I^0(\Phi)$. Consequently, the values of $\Delta G_I^0(\Phi)$ and grain boundary concentrations (according to eq. (8)) for *any* element at *any* grain boundary at *any* temperature for *any* bulk concentration (supposing the conditions necessary for derivation of eq. (8) are fulfilled) can be determined. The predicted values of ΔH_I^0 and ΔS_I^0 for selected elements are given in Table 2. The agreement between the predicted values of ΔH_I^0 and ΔS_I^0 for Al, Cr, Ni, P, Sb and Sn segregation in α-iron and those found in literature is surprisingly good as can also be seen from Fig. 5. In addition, the predicted concentrations of boron (5.4at.%B at 673 K) and sulphur (8.6at.%S at 823 K) at general grain

boundaries in respective binary systems with α-iron are also in excellent agreement with the experimental data found for polycrystalline alloys (4at.%B and 6at.%S at corresponding temperatures) [12,19].

Table 1 Parameters needed for prediction of grain boundary segregation (eqs. (16) and (21)) in α-iron [12,19]. The parameters were determined from the measurements of silicon, phosphorus and carbon segregation at individual grain boundaries in α-iron [9,11]

	$\Delta H_I^*(\Phi)$	v	$\Delta S'$ (J/(mol.K))	T_c (K)
General grain boundaries	**–8 to –4**	0.77		
Vicinal grain boundaries	**–2 to +2**	0.77		
Special grain boundaries	**+5 to +8**	0.77		
Substitution segregation			+5	930
Interstitial segregation			+56	930

Table 2 Selection of predicted values of the enthalpy and entropy of segregation of various solutes at individual grain boundaries in α-iron (S – substitution, I – interstitial) [12,19]. The data on solid solubility of the solute elements in α-iron were taken from [20]

solute	solubility [20]		site	ΔH_I^0 (kJ/mol) / ΔS_I^0 (J/(mol.K))		
	X_I^*	T (K)		{013} (special) ΔH^* = +6 kJ/mol	(001)/(034) (vicinal) ΔH^* = +2 kJ/mol	45°[100], (general) ΔH^* = –6 kJ/mol
Al	0.2	718	S	–1 / +4	–5 / –1	–13 / –9
As	0.095	1173	I	–12 / +43	–16 / +39	–24 / +31
B	0.00005	1185	I	–69 / –20	–73 / –24	–81 / –33
C	0.001013	1000	I	–38 / +15	–42 / +11	–50 / +2
Co	0.75	1008	S	0 / +5	0 / +5	–8 / –4
Cr	0.37	1073	S	–1 / +4	–5 / 0	–13 / –9
Cu	0.018	1130	S	–23 / –20	–27 / –24	–35 / –33
H	0.0001	995	I	–53 / –1	–57 / –5	–65 / –14
Mg	0.0004	1185	S	–53 / –53	–57 / –57	–65 / –65
Mn	0.03	873	S	–14 / –10	–18 / –14	–26 / –23
Mo	0.055	1173	S	–16 / –12	–20 / –16	–28 / –25
N	0.004	864	I	–25 / +30	–29 / +25	–37 / +17
Nb	0.007	1234	S	–33 / –31	–37 / –35	–45 / –44
Ni	0.058	748	S	–8 / –4	–12 / –8	–20 / –16
O	0.000008	1185	I	–83 / –33	–87 / –38	–95 / –46
P	0.033	1173	I	–20 / +35	–24 / +31	–32 / +22
S	0.00033	1200	I	–56 / –4	–60 / –8	–68 / –17
Sb	0.0419	1173	I	–18 / +37	–22 / +33	–30 / +24
Si	0.305	1313	S	–4 / +1	–8 / –4	–16 / –12
Sn	0.095	1183	I	–12 / +43	–16 / +39	–24 / +30
Ti	0.0308	1173	S	–20 / –17	–24 / –21	–32 / –29
V	0.25	1178	S	–4 / 0	–8 / –4	–16 / –13
W	0.02	1173	S	–23 / –20	–27 / –24	–35 / –33

Let us now apply this prediction to complex α-iron based systems such as low-alloy ferrite steel and ferrite phase of nodular cast iron, where intergranular decohesion may also occur (Fig. 6). Although the nominal compositions of these systems is well known, it is necessary to find the *real* concentrations of individual solutes *dissolved* in ferrite matrix of particular material at a chosen temperature. It is well known that a part of the solute atoms is usually bound in precipitates and thus, they do not participate in segregation equilibrium. An estimate of the ferrite composition in particular alloys may be calculated, for example, using the THERMO-CALC program [21,22]. In Tables 3 and 4 related to the chosen steel and nodular cast iron, respectively, the bulk content of solute elements are compared to their concentrations in ferrite.

In case of the steel (Table 3), we compared predicted values of grain boundary concentration, (${}^{P}X_I^{\Phi}$) with the experimental values (${}^{E}X_I^{\Phi}$) measured after equilibrium annealing at 853 K. The data in brackets are too low to be detected by Auger electron spectroscopy on intergranular fracture surfaces (AES). Carbon was not considered in determination of grain boundary composition (N) because its segregated portion is hardly distinguishable from that present in carbides as well as from that contaminated at the fracture surface during measurements.

The value of ${}^{E}X_P^{\Phi}$ is in excellent agreement with the value of ${}^{P}X_P^{\Phi}$ but the predicted and experimental data for chromium differ substantially. This difference may origin in the estimate of chromium concentration in bulk solid solution and/or in the quantification procedure of AES. The predicted concentrations of molybdenum and vanadium are low, and correspondingly they were not detected by AES. The concentrations of silicon and manganese are principally measurable by AES, however, the peaks of both elements are very close to those of iron and therefore, it is complicated to distinguish them for such low concentrations. Grain boundary concentration of carbon is under the detection limit of AES that justifies neglecting the measured peaks of carbon that originated mainly from the precipitates and contamination effects. In any case, it is remarkable that the method predicts (qualitatively at least) segregation of all solutes that was also measured experimentally. Nevertheless, for complete prediction it is necessary to take into account mutual interaction between solute elements as to correlate the value of ΔG_I^E (eq. (6)). Until now, however, there is no available way to predict these values.

Table 3 Comparison of predicted and experimental data for a low-alloy steel. W_I…nominal bulk concentrations; X_I^{sol}…calculated solute concentrations in ferrite at 853 K; ${}^{E}X^{\Phi}{}_I$…experimental values of grain boundary concentrations in polycrystals at 853 K; ${}^{P}X_I^{\Phi}$…solute concentrations at a general grain boundary at 853 K predicted for ideal multicomponent Fe–*I* system. The data in bold may be compared [12]

steel	Cr	Mo	V	Si	P	C	Mn	S	Ref.
W_I (mass.%)	2.48	0.03	0.01	0.32	0.011	0.12	0.68	0.008	[23]
X_I^{sol} (at.%)	1.63	0.016	0.0035	0.63	0.02	0.00065	0.68	0	
${}^{E}X_I^{\Phi}$ (at.%)	**15**	–	–	–	**19**	**N**	–	–	[12,23]
${}^{P}X_I^{\Phi}$ (at.%)	**2.7**	**(0.03)**	**(0.006)**	**1.1**	**19**	**(0.7)**	**1.3**	–	

Table 4 Comparison of experimental data for nodular cast iron D1248 with the predicted ones for 1073 K. For meaning of symbols see Table 3

cast iron D1248	C	Mn	Si	P	S	Cr	Mg	Ref.
W_I (mass.%)	3.73	0.30	2.80	0.069	0.016	0.02	0.042	[24]
X_I^{sol} (at.%)	0.074	0.230	6.034	0.120	0	0.0022	0.094	
${}^{E}X_I^{\Phi}$ (at.%)	**8**	**–**	**4**	**14**	**–**	**–**	**–**	[24]
${}^{P}X_I^{\Phi}$ (at.%)	**14**	**(0.1)**	**4.5**	**32**	–	**(0.02)**	**(0.1)**	

Grain boundary composition of ferrite phase in nodular cast iron D1248 was treated similarly (Table 4). As in case of the steel, sulphur is supposed to be completely precipitated in MnS and not participating in segregation. In contrast to the steel, the amount of carbon dissolved in ferrite is high enough to take its segregation into account. Additionally, the data of ${}^{E}X_{P}^{\Phi}$ in Table 4 were measured at grain boundaries of a slowly cooled material that was not tempered for segregation. It means that the segregation state at the boundary was not developed during changed temperatures and therefore, these data cannot be ascribed to a specific temperature. As it is seen from Table 4, the values of ${}^{P}X_{I}^{\Phi}$ and ${}^{E}X_{I}^{\Phi}$ are in good qualitative agreement: Grain boundary segregation at 1073 K was predicted for all solutes the segregation of which was found experimentally, i.e., for phosphorus, silicon and carbon. The predicted interfacial concentrations of manganese, chromium and magnesium are low, and correspondingly they were not detected by AES. One can expect that in equilibrium, the concentration of carbon and phosphorus should be higher and that of silicon lower than the measured values of ${}^{E}X_{I}^{\Phi}$. Due to dominant repulsive Si–P interaction, the content of silicon should be substantially suppressed. Nevertheless, elements as silicon, carbon and phosphorus will appear at grain boundaries in equilibrium whereas the other solutes present in the cast iron will not reach measurable concentrations at the grain boundaries [9].

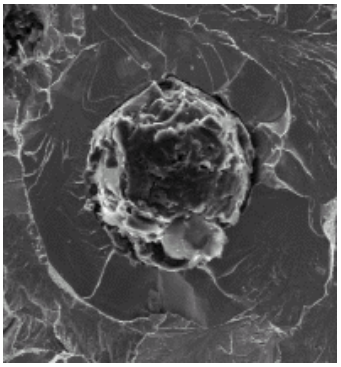

Fig.6 SEM micrograph taken in vicinity of a globular graphite particle showing intergranular decohesion in ferrite fractured prevailingly by cleavage. The arrow indicates the intergranular facet

Conclusions

Thermodynamic analysis of the effect of interfacial energy on grain boundary segregation revealed novel relationships between thermodynamic parameters of grain boundary segregation. The dependence of the standard molar enthalpy of segregation on both the solute solid solubility and the grain boundary structure resulted in construction of the grain boundary segregation diagram and in refinement of the earlier model of Hondros and Seah. It was also shown that all thermodynamic parameters of grain boundary segregation change with changing the interfacial energy evoked by changes of both the grain boundary structure and the nature of segregated element. The dependence of enthalpy and entropy of grain boundary segregation on interfacial energy can be represented by the compensation effect. Both relationships – the grain boundary segregation diagram and the compensation effect – were successfully used to predict grain boundary segregation of any element at any grain boundary in binary systems and in complex systems such as steels and cast irons, as well.

Acknowledgement

This work was supported by the grants of the Czech Science Foundation (202/06/0004) and of the Czech–Slovak bilateral co-operation (37/2006). The authors are grateful to Dr. Aleš Kroupa of IPM AS CR for providing assistance with calculations using THERMO-CALC program.

Literature

[1] Sutton A.P., Balluffi R.W.: *Interfaces in Crystalline Materials* (Clarendon, Oxford 1995).
[2] Hondros E.D., Seah M.P., Hofmann S., Lejček P: Interfacial and surface microchemistry. In: *Physical Metallurgy*, 4th ed, ed. by R.W. Cahn, P. Haasen (North–Holland, Amsterdam, 1996) pp. 1201–1289.
[3] Chang L.S., Rabkin E., Straumal B.B., Hofmann S., Baretzky B., Gust W.: Def. Diff. Forum 156, 135 (1998).
[4] Janovec J.: *Nature of Alloy Steel Intergranular Embrittlement* (Veda, Bratislava, 1999).
[5] Biloni H., Boetinger W.J.: Solidification. In: *Physical Metallurgy*, 4th ed., ed. by R.W. Cahn, P. Haasen (North–Holland, Amsterdam, 1996) pp. 669–842.
[6] duPlessis J., van Wyk G.N.: J. Phys. Chem. Solids 49, 1441 and 1451 (1988).
[7] duPlessis J.: Solid State Phenom. 11, 1 (1990).
[8] Gaskell D.R.: Metallurgical thermodynamics. In: *Physical Metallurgy*, 4th ed., ed. by R.W. Cahn, P. Haasen, (North-Holland, Amsterdam, 1996). pp. 413–469.
[9] Lejček P., Hofmann S.: Crit. Rev. Mater. Sci. Sol. State 20, 1 (1995).
[10] Lejček P.: Z. Metallkde 96, 1129 (2005).
[11] Lejček P., Hofmann S., Paidar V.: Acta Mater. 51, 3951 (2003).
[12] Lejček P., Hofmann S., Janovec J.: Mater. Sci. Eng. A, in press.
[13] Hondros E.D., Seah M.P.: Metall. Trans. A 8, 1363 (1977).
[14] Lejček P., Hofmann S.: Interface Sci. 1, 163 (1993).
[15] *Selected Values of the Thermodynamic Properties of Binary Alloys*, ed. by R. Hultgren, P. Desai, D. Hawkins, M. Gleiser, K. Kelley (ASM, Metals Park, 1973).
[16] Watanabe T., Kitamura S., Karashima S.: Acta Metall. 28, 455 (1980).
[17] Lejček P.: Z. Metallkde, 96, 1129 (2005).
[18] Rubinovich L., Polak M: Europ. Phys. J. B 22, 267 (2001).
[19] Lejček P., Hofmann S.: Grain boundary segregation, anisotropy and prediction, In: *Encyclopedia of Materials: Science and Technology – Updates*, ed. by K. Bunshaw, R.W. Cahn, M. Flemings, E. Kramer, S. Mahajan (Pergamon, Amsterdam, 2002) #200115, pp. 1–7.
[20] Kubaschewski O.: *Iron – Binary Phase Diagrams* (Springer, Berlin, 1982); Massalski, T.B.: *Binary Alloy Phase Diagrams* (ASM, Metals Park, 1987); Predel, B.: *Phase Equilibria of Binary Alloys* (Springer, Berlin, 2003).
[21] Sundman B.: THERMO-CALC, version L (Royal Inst. Technol., Stockholm, 1997).
[22] Kroupa A., Havránková J., Coufalová M., Svoboda M., Vřešťál J.: J. Phase Equil. 22, 312 (2001).
[23] Janovec J., Grman D., Perháčová J., Lejček P., Patscheider J., Ševc P.: Surf. Interface Anal. 30, 354 (2000).
[24] Konečná R., Lejček P., Nicoletto G., Bartuška P.: Mater. Sci. Tech., in press.